J. Plasma Physics (2008), *vol.* 74, *part* 4, *pp.* 555–568. © 2008 Cambridge University Press
doi:10.1017/S002237780800706X Printed in the United Kingdom

Small-amplitude analysis of a non-thermal variable charge dust soliton

MOULOUD TRIBECHE

Plasma Physics Group, Theoretical Physics Laboratory, Faculty of Sciences-Physics, University of Bab-Ezzouar, USTHB, B.P. 32, El Alia, Algiers 16111, Algeria (mouloudtribeche@yahoo.fr)

(Received 5 August 2007 and accepted 27 November 2007, first published online 28 February 2008)

Abstract. Small-amplitude electrostatic solitary waves are investigated in an unmagnetized dusty plasma with hot variable charge non-thermal dust grains. These nonlinear localized structures are small-amplitude self-consistent solutions of the Vlasov equation in which the dust response is non-Maxwellian. Localized solitary structures that may possibly occur are discussed and the dependence of their characteristics on physical parameters is traced. Our investigation may be taken as a prerequisite for the understanding of the electrostatic solitary waves that may occur in space dusty plasmas.

1. Introduction

A dusty plasma is a normal electron–ion plasma with an additional highly charged component of small micrometer or sub-micrometer-sized extremely massive charged particulates (dust grains) [1–5]. The dust particles are many orders of magnitude heavier than ions, are a source of ionization and recombination for electrons, and their charge is not fixed, but depends on local plasma parameters. Wave propagation in such complex systems is therefore expected to be substantially different from the ordinary two-component plasmas and the presence of charged dust can have a strong influence on the characteristics of the usual plasma wave modes, even at frequencies where the dust grains do not participate in the wave motion. Recently, there has been a rapidly growing interest in the study of different types of collective processes in dusty plasmas because of their relevance and vital role in laboratory, space, and astrophysical plasma environments, such as cometary tails, asteroid zones, planetary rings, interstellar medium, the Earth's ionosphere and magnetosphere, etc. Dust also occurs in laboratory plasmas, including those used for materials processing [6]. Waves in dusty plasmas have been studied theoretically for about two decades, beginning with the work of Bliokh and Yarashenko [7] on electrostatic waves in Saturn's rings. Dusty plasmas are known to support a wide variety of ultra-low-frequency wave modes [8, 9]. The most well studied of such modes are the so-called dust-acoustic wave (DAW) [10] and dust–ion-acoustic wave (DIAW) [11,12]. The DIAW is the usual ion-acoustic mode modified by the presence of dust particles and the DAW arises due to the restoring force provided by the plasma thermal pressure while the inertia is due to the dust mass. The DAW/DIAW propagate as linear normal modes when the phase velocity is much larger than the dust thermal velocity. However, there are numerous processes via which unstable

https://doi.org/10.1017/S002237780800706X Published online by Cambridge University Press

modes can saturate and attain large amplitude [13–24]. When the amplitudes of the waves are sufficiently large, nonlinearities cannot be ignored. They come from the harmonic generation involving the fluid advection, the nonlinear Lorentz force, trapping of particles in the wave potential, the ponderomotive force, etc. The nonlinearities in plasmas contribute to the localization of waves, leading to different and interesting nonlinear coherent structures (solitary structures, shock waves, vortices, etc.). These coherent structures may play the role of basic nonlinear elements in phenomena such as turbulence, heating, transport, etc., and hence their properties are of fundamental interest. Nonlinear DAWs and DIAWs of large and small amplitude have been studied extensively in recent years [25–49]. The analysis have been derived on the basis of the Sagdeev quasi-potentials or the reductive perturbation theory, which leads to the dynamical system being described by the Korteweg–de Vries (KdV) or derivative nonlinear Schrödinger (NLS) type equations.

The aim of the present paper is to present a theoretical model to show the existence and formation of small-amplitude electrostatic solitary potentials in a dusty plasma with variable charge hot non-thermal dust grains. These nonlinear localized structures are small-amplitude self-consistent solutions of the Vlasov equation representing saturated states of a three-stream unstable collisionless dusty plasma. The saturation is provided by an interplay between dust particle non-thermality and dust charging. It is worth noting that some recent theoretical work has focused on the effects of non-thermal electrons and ions, which are common in space plasmas [50–56]. The outline of this paper is as follows. In the next section, we present the basic equations of the theoretical model where a small-amplitude analysis is carried out. Our results are presented and discussed in Sec. 3. A summary of our results and conclusions is given in Sec. 4.

2. Basic equations

2.1. Constant dust charge case

Let us consider an unmagnetized dusty plasma having electrons, positive ions, and dust grains of density $n_{\rm e}$, $n_{\rm i}$, and $n_{\rm d}$, respectively. We assume for simplicity that all the grains have the same charge, equal to $q_{\rm d} = -eZ$, with Z positive for negatively charged dust and negative for positively charged dust. All the dust grains are assumed to have the same size and to be spheres of radius r. On the dust timescale, the electrons and ions are assumed to be in thermal equilibrium, with densities

$$n_j = n_{j0} \exp\left(-\frac{q_j \phi}{T_j}\right) \tag{1}$$

where $j = {\rm e}, {\rm i}$ denote electrons and ions, respectively, ϕ is the electrostatic potential, $q_{j={\rm e,i}} = \mp e$ are the charges, and T_j the temperatures. The subscript 0 stands for equilibrium values. To model the hot dust distribution with a population of fast particles, we can refer to an appropriate Bernstein–Greene–Kruskal (BGK) solution which solves the dust Vlasov equation [50]. Thus, we choose

$$f_{\rm d}(x, v_{\rm d}) = \frac{n_{\rm d0}}{1+3\alpha}\left(\frac{m_{\rm d}}{2\pi T_{\rm d}}\right)^{1/2}\left\{1+2\alpha\left(\frac{m_{\rm d}v_{\rm d}^2/2 - Ze\phi}{T_{\rm d}}\right)\right\}\exp\left(-\frac{m_{\rm d}v_{\rm d}^2/2 - Ze\phi}{T_{\rm d}}\right). \tag{2}$$

Here α is a parameter determining the non-thermal dust particles present in our

https://doi.org/10.1017/S002237780800706X Published online by Cambridge University Press

plasma model. With distribution (2) we get

$$n_{\rm d}(\phi) = \int_{-\infty}^{+\infty} f_{\rm d}(x, v_{\rm d})\, dv_{\rm d} = n_{\rm d0}\left\{1 + \beta\left(\frac{Z^2 e^2 \phi^2}{T_{\rm d}^2} - \frac{Ze\phi}{T_{\rm d}}\right)\right\} \exp\left(\frac{Ze\phi}{T_{\rm d}}\right) \tag{3}$$

where

$$\beta = \frac{4\alpha}{1 + 3\alpha}. \tag{4}$$

Poisson's equation then becomes

$$\frac{d^2\Psi}{dX^2} = \exp(\Psi) - f\exp(-\sigma\Psi) + (f-1)N_{\rm d} \tag{5}$$

where

$$N_{\rm d} = n_{\rm d}/n_{\rm d0} = (1 - \beta\gamma\Psi + \beta\gamma^2\Psi^2)\exp(\gamma\Psi) \tag{6}$$

and $f = n_{\rm i0}/n_{\rm e0}$, $\sigma = T_{\rm e}/T_{\rm i}$ and $\gamma = Z(T_{\rm e}/T_{\rm d})$. The following normalized quantities $\Psi = e\phi/T_{\rm e}$ and $X = x/\lambda_{\rm De}$ are introduced and $\lambda_{\rm De} = (T_{\rm e}/4\pi n_{\rm e0}e^2)^{1/2}$ is the electron Debye length. Charge neutrality at equilibrium requires $1 - f + Z_0 n_{\rm d0}/n_{\rm e0} = 0$. Multiplying both sides of (5) by $d\Psi/dX$, and integrating once, we obtain the quadrature

$$\frac{1}{2}\left(\frac{d\Psi}{dX}\right)^2 + V(\Psi) = 0 \tag{7}$$

where the Sagdeev potential for our purpose reads as

$$V(\Psi) = -\exp(\Psi) - \frac{f}{\sigma}\exp(-\sigma\Psi) + \frac{\beta(1-f)}{\gamma}(\gamma^2\Psi^2 - 3\gamma\Psi + 3 + 1/\beta)\exp(\gamma\Psi) + C, \tag{8}$$

with C the constant of integration. Making use of the boundary condition $V(\Psi = 0) = 0$, we obtain

$$C = 1 + \frac{f}{\sigma} + \frac{(f-1)(3\beta+1)}{\gamma}. \tag{9}$$

Prior to the numerical solution, it is instructive to discuss the conditions under which (7) leads to soliton solutions of arbitrary amplitude by analyzing the Sagdeev potential. It is clear from (8) that $V(\Psi) = 0$ and $dV(\Psi)/d\Psi = 0$ at $\Psi = 0$. Solitary wave solutions of (7) exist if [25] (i) $(d^2V/d\Psi^2)_{\Psi=0} \prec 0$, so that the fixed point at the origin is unstable, (ii) there exists a non-zero $\Psi_{\rm m}$, the maximum (or minimum) value of Ψ, at which $V(\Psi_{\rm m}) \succeq 0$, and (iii) $V(\Psi) \prec 0$ when Ψ lies between 0 and $\Psi_{\rm m}$. The second condition simply means that a quasiparticle of zero total energy will be reflected at the position $\Psi = \Psi_{\rm m}$. The third condition means that V has to be a potential trough in which the quasiparticle can be trapped and experience oscillations. Condition (i) for the existence of electrostatic localized structures requires the plasma parameters to satisfy

$$1 + \sigma f + (f-1)\gamma(1-\beta) > 0. \tag{10}$$

It is obvious that the conditions for the existence of solitary waves depend sensitively on the plasma parameters. In the following, instead of proving directly the existence of large but finite-amplitude solitary solutions, which would mean solving numerically (7), we first perform the analysis for small amplitudes. In the small-amplitude limit, $\Psi \ll 1$, the nature of the solution to (7) may be obtained explicitly.

https://doi.org/10.1017/S002237780800706X Published online by Cambridge University Press

Expanding in Ψ and retaining leading-order terms, we find that (7) reduces to

$$V(\Psi) = A_1\Psi^2 + A_2\Psi^3 + 0(\Psi^4) \tag{11}$$

where

$$A_1 = \tfrac{1}{2}\{\gamma(f-1)(\beta-1) - f\sigma - 1\},$$

$$A_2 = \tfrac{1}{6}\{-\gamma^2(f-1) + f\sigma^2 - 1\}. \tag{12}$$

Performing the last step in deriving the soliton solutions, namely solving the 'energy equation' (7), one gets

$$\begin{aligned}\Psi(X) &= \Psi_M \operatorname{sech}^2[(X - X_0)/\Delta] \\ &= -\frac{A_1}{A_2}\operatorname{sech}^2\left[\sqrt{-\frac{A_1}{2}}(X - X_0)\right] \\ &= \Psi_M \operatorname{sech}^2\left[\sqrt{\frac{A_2}{2}\Psi_M}(X - X_0)\right].\end{aligned} \tag{13}$$

Solution (13) represents a small-amplitude stationary solitary wave provided $A_1 \prec 0$ or

$$\frac{\gamma(f-1)(\beta-1)}{1+f\sigma} < 1.$$

The potential form (13) deviates from that of the usual KdV soliton, which is given by

$$\Psi(X) = \Psi_M \operatorname{sech}^2[\sqrt{\tfrac{1}{6}\Psi_M}(X - X_0)] \tag{14}$$

in the scaling of the sech argument. Now retaining terms up to Ψ^4, (11) may be expanded as

$$V(\Psi) = A_1\Psi^2 + A_2\Psi^3 + A_3\Psi^4 + \mathrm{O}(\Psi^5), \tag{15}$$

where

$$A_3 = \tfrac{1}{24}\{-f\sigma^3 - (f-1)\gamma^3(3\beta+1) - 1\}. \tag{16}$$

Integrating (7), we get

$$\begin{aligned}\Psi(X) &= \frac{1}{(A_2^2/4A_1^2 - A_3/A_1)^{1/2}\cosh[\sqrt{-2A_1}(X - X_0)] - A_2/2A_1} \\ &= \frac{1}{(A_2^2/4A_1^2 - A_3/A_1)^{1/2}[2\cosh^2(\sqrt{-2A_1}(X - X_0)/2) - 1] - A_2/2A_1}.\end{aligned} \tag{17}$$

Solution (17) represents a small-amplitude stationary solitary wave provided $A_1 \prec 0$ and $A_2^2/4A_1^2 \succ A_3/A_1$.

2.2. Variable dust charge case

We now discuss the variable dust charge case. The dust particles are described by the coupled set of Vlasov–Poisson equations. Accordingly, in order to solve the Vlasov equation for dust particles with variable charge, we make use of an appropriate ansatz in terms of the constants of motion. To model the hot dust distribution in the presence of trapped particles, we refer to an appropriate BGK solution. Since

https://doi.org/10.1017/S002237780800706X Published online by Cambridge University Press

the dust charge is allowed to change, we rewrite $E_{\rm d}$ as

$$E_{\rm d} = \frac{1}{2} m_{\rm d} v_{\rm d}^2 + \int_0^{\phi} q_{\rm d}\, d\phi, \tag{18}$$

so that $E_{\rm d}$ becomes a constant of the motion and thus $f(E_{\rm d})$ satisfies the stationary Vlasov equation. Thus, we have

$$f_{\rm d}(x, v_{\rm d}) = \frac{n_{\rm d0}}{1+3\alpha}\left(\frac{m_{\rm d}}{2\pi T_{\rm d}}\right)^{1/2}\left\{1 + 4\alpha\left(\frac{m_{\rm d} v_{\rm d}^2/2 + \int_0^{\phi} q_{\rm d}\, d\phi}{T_{\rm d}}\right)\right\}$$

$$\times \exp\left(-\frac{m_{\rm d} v_{\rm d}^2/2 + \int_0^{\phi} q_{\rm d} Z\, d\phi}{T_{\rm d}}\right). \tag{19}$$

With distribution (19) we get

$$n_{\rm d}(\phi) = n_{\rm d0}\left\{1 + \beta\left(\frac{(\int_0^{\phi} q_{\rm d}\, d\phi)^2}{T_{\rm d}^2} + \frac{\int_0^{\phi} q_{\rm d}\, d\phi}{T_{\rm d}}\right)\right\}\exp\left(-\frac{\int_0^{\phi} q_{\rm d}\, d\phi}{T_{\rm d}}\right) \tag{20}$$

or

$$N_{\rm d} = n_{\rm d}/n_{\rm d0} = \{1 + \beta(\alpha_1^2\xi^2 + \alpha_1\xi)\}\exp(-\alpha_1\xi), \tag{21}$$

where

$$\xi = \int_0^{\Psi} Q_{\rm d}\, d\Psi \tag{22}$$

and

$$\alpha_1 = r T_{\rm e}^2/e^2 T_{\rm d}, \quad Q_{\rm d} = \frac{e q_{\rm d}}{r T_{\rm e}}. \tag{23}$$

The Poisson equation becomes

$$\frac{d^2\Psi}{dX^2} = \exp(\Psi) - f\exp(-\sigma\Psi) + \frac{(f-1)}{Q_{\rm d0}} Q_{\rm d} N_{\rm d}. \tag{24}$$

Multiplying both sides of (24) by $d\Psi/dX$ and integrating once, we obtain the quadrature

$$\frac{1}{2}\left(\frac{d\Psi}{dX}\right)^2 + V(\Psi) = 0, \tag{25}$$

where the Sagdeev potential for our purpose reads as

$$V(\Psi) = -\exp(\Psi) - \frac{f}{\sigma}\exp(-\sigma\Psi) - \frac{(f-1)}{Q_{\rm d0}}\int_0^{\Psi} Q_{\rm d} N_{\rm d}\, d\Psi. \tag{26}$$

In the standard orbit-limited probe model for the dust grain [57], the latter is charged by the plasma currents at the grain surface. The charging current originates from electrons and ions hitting the grain surface. Accordingly, the variable dust charge $q_{\rm d} = -eZ$ is determined self-consistently by (note that we consider a one-dimensional stationary plasma)

$$v_{\rm d}\frac{dq_{\rm d}}{dx} = I_{\rm e} + I_{\rm i}, \tag{27}$$

where $I_{\rm e}$ and $I_{\rm i}$ are the average microscopic electron and ion currents entering the dust grains. The grain current from the Boltzmann electrons and ions are [58–60]

$$I_j = \pi r^2 q_j (8T_j/\pi m_j)^{1/2} n_j W_j, \tag{28}$$

https://doi.org/10.1017/S002237780800706X Published online by Cambridge University Press

where $r \ll \lambda_{De}$ is the grain radius and m_j are the masses. For $q_d < 0$, we have [61,62]

$$W_e = \exp(eq_d/rT_e) \tag{29}$$

and

$$W_i = 1 - eq_d/rT_i. \tag{30}$$

We assume that the cold dust grains, whose masses are much greater than those of the ions, are accelerated by a weak presheath field to a velocity v_{d0}. Thus the number conservation equation, after integration, yields

$$n_d v_d = n_{d0} v_{d0}. \tag{31}$$

After rearranging the terms in (27), one can obtain the following normalized charging equation:

$$\frac{dQ_d}{dX} = kN_d \left\{ -\exp(\Psi + Q_d) + \sqrt{\frac{\mu}{\sigma}} f \exp(-\sigma\Psi)(1 - \sigma Q_d) \right\}, \tag{32}$$

with k given by

$$k = \sqrt{\frac{2n_{e0}e^2r^2}{m_e v_{d0}^2}} \tag{33}$$

and $\mu = m_e/m_i$. Equation (32) is the additional dynamical equation that is coupled to the plasma equations through the plasma currents. The dust electric charge becomes a dynamical variable which is coupled self-consistently to the other dynamical variables such as density and potential. Charge neutrality at equilibrium ($\Psi = 0$) requires the following constraint:

$$f = \sqrt{\frac{\sigma}{\mu}} \frac{\exp(Q_{d0})}{1 - \sigma Q_{d0}}. \tag{34}$$

In the following numerical simulation, the value of f is deduced from the above relation while the remaining other parameters ($Q_{d0}, r, T_e, \sigma, T_{df}, \beta, \mu, n_{i0}$ and v_{d0}) are given first. We note that the characteristic time for dust motion is of the order of tens of milliseconds for micrometer-sized grains, while the dust charging time is typically of the order of 10^{-8} s. Within the time of charging, the displacement of the grain is thus negligible compared to the spatial scale of the problem. It follows that the charging process can be treated as a local phenomenon, and the convective term which appears on the left-hand side of the usual charging equation can be neglected. It follows that we have

$$I_e + I_i \simeq 0 \tag{35}$$

and the grains are always at the floating potential. Thus, (32) leads to

$$(1 + \sigma)\Psi = \ln\left\{ \frac{1 - \sigma Q_d}{1 - \sigma Q_{d0}} \exp(Q_{d0} - Q_d) \right\}. \tag{36}$$

Neglecting terms of $O(\sigma^{-1})$ we obtain the following transcendental relation between Ψ and Q_d:

$$\sigma\Psi = Q_{d0} - Q_d + \ln \frac{Q_d}{Q_{d0}}. \tag{37}$$

https://doi.org/10.1017/S002237780800706X Published online by Cambridge University Press

Assuming that the relative variation of the charge is sufficiently small and expanding $\ln(Q_{\rm d}/Q_{\rm d0}) \simeq (Q_{\rm d} - Q_{\rm d0})/Q_{\rm d0}$, we obtain

$$\frac{Q_{\rm d}}{Q_{\rm d0}} = 1 - \frac{\sigma\Psi}{Q_{\rm d0} - 1} \tag{38}$$

and it becomes possible to perform the potential energy integral

$$\xi = \int_0^{\Psi} Q_{\rm d}\, d\Psi = Q_{\rm d0}\left[\Psi - \frac{\sigma\Psi^2}{2(Q_{\rm d0} - 1)}\right]. \tag{39}$$

In the small-amplitude limit, $\Psi \ll 1$, the nature of the solution of (24) may be obtained explicitly. Expanding in Ψ and retaining leading-order terms, we find that (21) and (26) reduce respectively to

$$N_{\rm d} = 1 + \alpha_1 Q_{\rm d0}(\beta - 1)\Psi + \frac{\alpha_1 Q_{\rm d0}}{2(Q_{\rm d0} - 1)}(\sigma + \alpha_1 Q_{\rm d0}^2 - \alpha_1 Q_{\rm d0} - \beta\sigma)\Psi^2 + {\rm O}(\Psi^3) \tag{40}$$

and

$$V(\Psi) = B_1\Psi^2 + B_2\Psi^3, \tag{41}$$

where

$$B_1 = -\frac{1}{2}\left\{1 + f\sigma - (f-1)\alpha_1 Q_{\rm d0} + (f-1)\beta\alpha_1 Q_{\rm d0} - \frac{(f-1)\sigma}{Q_{\rm d0} - 1}\right\},$$

$$B_2 = -\frac{1}{3}\left\{\frac{1}{2} - \frac{f\sigma^2}{2} + \frac{(f-1)\alpha_1 Q_{\rm d0}}{2(Q_{\rm d0} - 1)}(-\sigma + \alpha_1 Q_{\rm d0}^2 - \alpha_1 Q_{\rm d0} - 3\beta\sigma)\right\}. \tag{42}$$

Performing the last step in deriving the soliton solutions, namely solving the 'energy equation' (25), one gets

$$\Psi(X) = -\frac{B_1}{B_2}\,{\rm sech}^2\left[\sqrt{-\frac{B_1}{2}}(X - X_0)\right]. \tag{43}$$

Solution (43) represents a small-amplitude stationary solitary wave provided $B_1 < 0$. It is obvious that the conditions for the existence of localized structures depend sensitively on the dust non-thermal parameter β. We note that, in the dust free case ($f = 1$), solution (43) reduces to

$$\Psi(X) = \frac{3}{(\sigma - 1)}\,{\rm sech}^2\left[\frac{\sqrt{1+\sigma}}{2}(X - X_0)\right]. \tag{44}$$

3. Discussion

Solution (43) represents a small-amplitude stationary solitary wave provided $B_1 < 0$ and $B_2^2/4B_1^2 > B_3/B_1$. For the sake of comparison, we have plotted the spatial variation of Ψ for various values of $Q_{\rm d0}$. The electrostatic potential Ψ exhibits a spatially localized structure as is evident from Fig. 1. The parameters $T_{\rm e} = 2$ eV, $\sigma = 2$, $r = 10^{-2}$ μm, $\alpha = 0.5$, $n_{\rm i0} = 10^8$ cm^{-3} and $T_{\rm d} = T_{\rm i}/10$ have been chosen so that the conditions for the existence of small-amplitude solitary solutions are fulfilled. It can be seen that as $Q_{\rm d0}$ increases ($Q_{\rm d0}$ becomes least negative) the height as well as the width of the soliton decrease. When Q_{d0} passes a certain critical value (Fig. 2), the tendency is reversed: the pulse amplitude increases while its width decreases, i.e. an increase of $Q_{\rm d0}$ makes the solitary structure more spiky. With an increase of the grain radius r (Fig. 3), the height and the width of the soliton decrease. A decrease of the dust temperature $T_{\rm d}$ (Fig. 4) would lead to

https://doi.org/10.1017/S002237780800706X Published online by Cambridge University Press

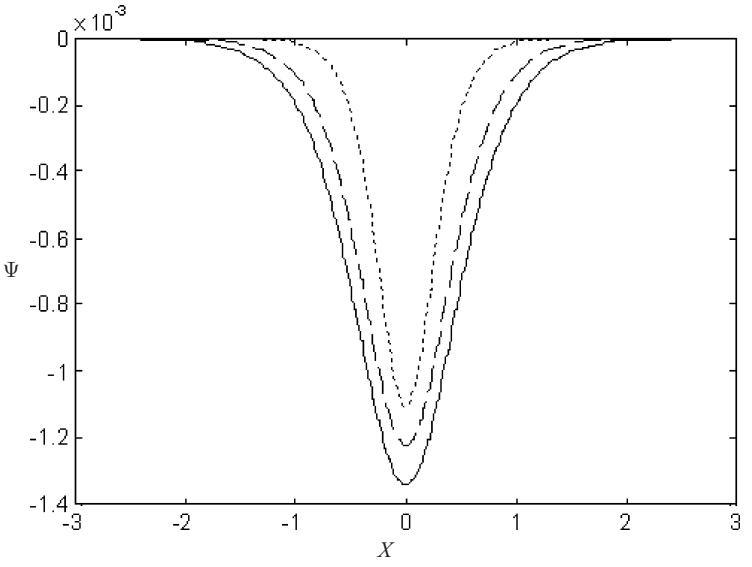


Figure 1. Small-amplitude soliton solution for the electrostatic potential Ψ for different values of $Q_{d0} = -2.32$ (solid curve, $f = 1.05$), -2.3 (dashed curve, $f = 1.08$) and -2.2 (dotted curve, $f = 1.24$) with $T_e = 2$ eV, $\sigma = 2$, $r = 10^{-2}$ μm, $\alpha = 0.5, n_{i0} = 10^8$ cm^{-3}, and $T_d = T_i/10$.

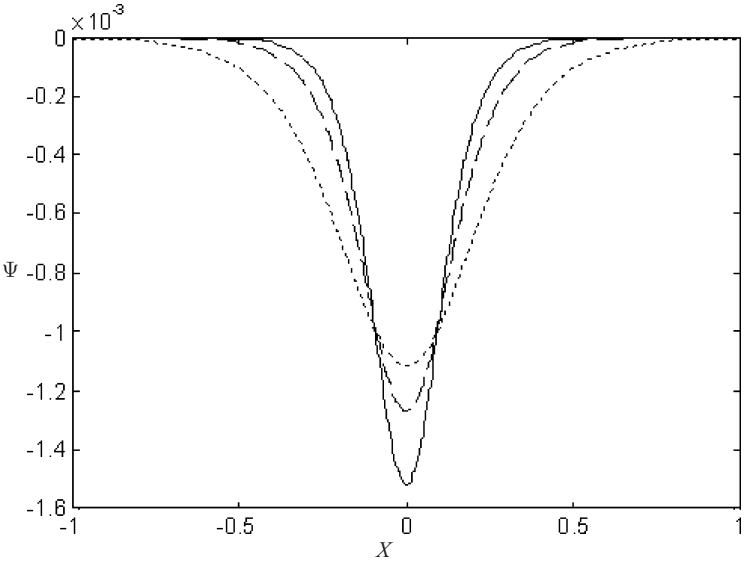


Figure 2. Small-amplitude soliton solution for the electrostatic potential Ψ versus X for different values of $Q_{d0} = -1.5$ (solid curve, $f = 3.38$), -1.8 (dashed curve, $f = 2.17$) and -2.1 (dotted curve, $f = 1.42$). The values of the remaining parameters are those used for Fig. 1.

a decrease of the pulse as well as the width of the solitary structure. Figure 5 reveals that the spatial patterns of the electrostatic solitary wave are significantly modified by the presence of non-thermal dust grains. With an increase of the

https://doi.org/10.1017/S002237780800706X Published online by Cambridge University Press

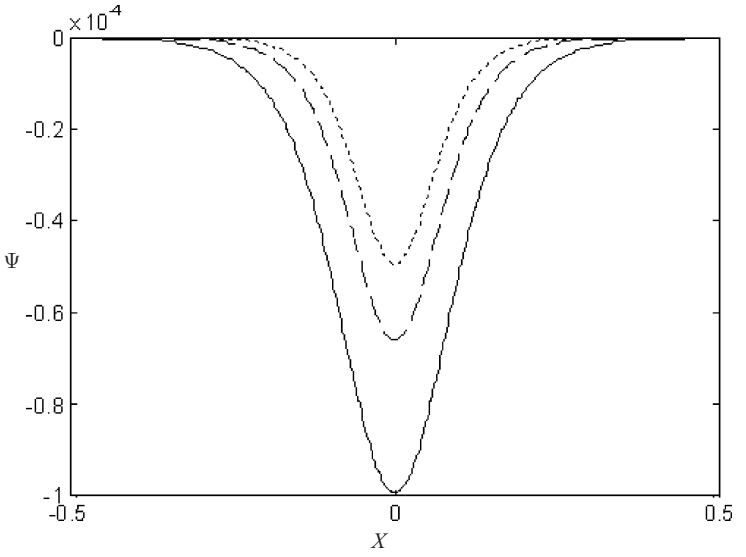


Figure 3. Small-amplitude soliton solution for the electrostatic potential Ψ versus X for different values of the grain radius $r = 0.1$ μm (solid curve), 0.15 μm (dashed curve) and 0.2 μm (dotted curve) with $T_e = 2$ eV, $\sigma = 2, Q_{d0} = -2.2, \alpha = 0.5, n_{i0} = 10^8$ cm^{-3} and $T_d = T_i/10$. The value of f deduced from (34) is 1.2434.

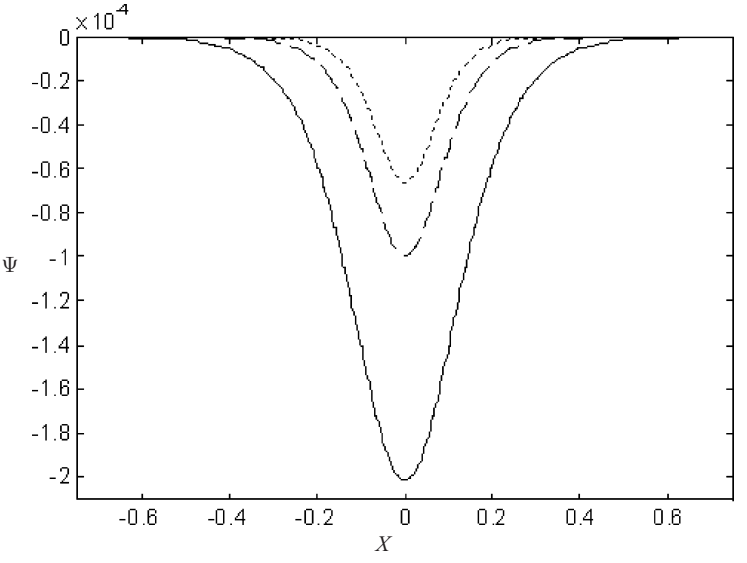


Figure 4. Small-amplitude soliton solution for the electrostatic potential Ψ versus X for different values of the grain temperature $T_d = T_i/5$ (solid curve), $T_i/10$ (dashed curve) and $T_i/15$ (dotted curve). The values of the remaining parameters are those used for Fig. 3 with $r = 0.1$ μm.

non-thermal parameter α, the pulse amplitude decreases while its width increases, i.e. the fast non-thermal dust grains make the solitary structure less spiky. The dust grain charge becomes least negative (Fig. 6) as the non-thermal parameter

https://doi.org/10.1017/S002237780800706X Published online by Cambridge University Press

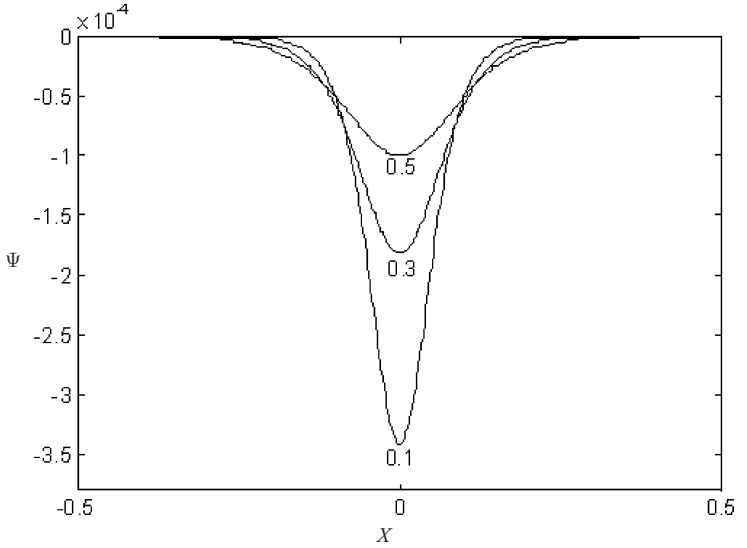


Figure 5. Small-amplitude soliton solution for the electrostatic potential Ψ versus X for different values of the nonthermal parameter α. The values of the remaining parameters are those used for Fig. 4 with $T_{\rm d} = T_{\rm i}/10$. The values of α are indicated on the figure.

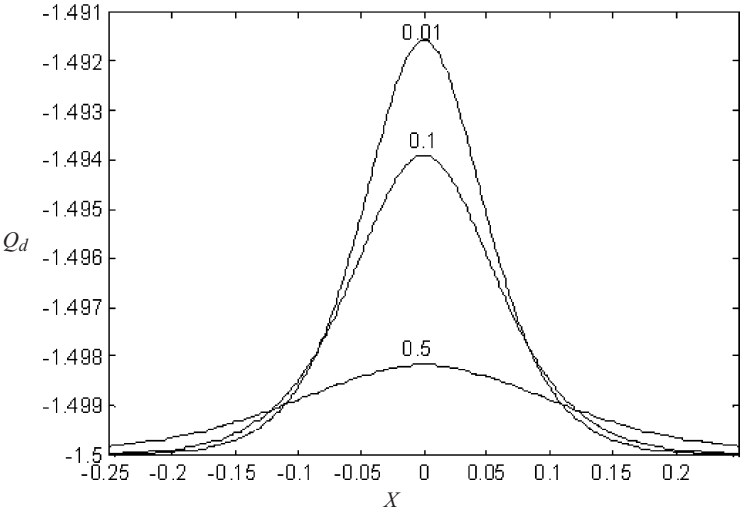


Figure 6. The spatial profile of the dust grain charge $Q_{\rm d}$ for different values of the non-thermal parameter α with $T_{\rm e} = 2$ eV, $\sigma = 2$, $r = 10^{-2}$ μm, $Q_{\rm d0} = -1.5$, $n_{\rm i0} = 10^8$ cm^{-3} and $T_{\rm d} = T_{\rm i}/10$. The value of f deduced from (34) is 3.3803. The values of α are indicated on the figure.

α decreases. The dust density (Fig. 7) is found to be highly localized with a void (hole) on each side of the density pulse. This localization (accumulation) is caused by a balance of the electrostatic forces on the dust grains. Figure 7 indicates that these dust voids enlarge when the non-thermal parameter α decreases. Finally, it may be useful to note that in the limit when the dust grains are closest (high dust number density regime), strong coupling effects such as dust–dust correlations

https://doi.org/10.1017/S002237780800706X Published online by Cambridge University Press

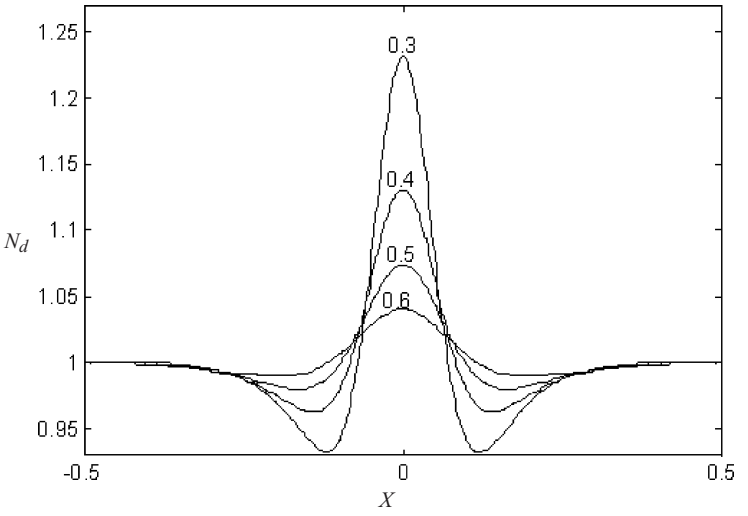


Figure 7. The spatial profile of the dust grain density N_{d} for different values of the non-thermal parameter α. The values of the remaining parameters are those used for Fig. 6. The values of α are indicated on the figure.

become important [63] and the dust particle potential is not equal to the floating potential.

4. Conclusion

To conclude, we have addressed the problem of low-frequency, small-amplitude electrostatic solitary structures in a dusty plasma with hot variable charge non-thermal dust grains. The influence of dust non-thermality, in addition to dust charge variation, on the conditions for the existence and formation of these small-amplitude solitary waves is discussed. Localized solitary structures that may possibly occur are discussed and the dependence of their characteristics on physical parameters is traced. Our results show that in such a plasma small-amplitude spatially localized structures, the height and nature of which depend sensitively on the non-thermal parameter α, can exist. However, their stability is far from easy to prove. We have then limited ourselves to finding localized structure solutions producing indirect evidence of their possible realization. Finally, some comments on the present analysis are in order. While the analysis can be carried out by including some relevant processes (such as ionization, diffusion, particle attachment, dissipation due to electron and ion elastic collisions with dust particles as well as charging collision with dust particles, etc.), we used, to keep the nonlinear analysis more tractable, some reasonable assumptions. On the extremely slow dust timescale, the electrons and ions are assumed to be in local thermodynamic equilibrium (their number densities obey the Boltzmann distribution) even when the grain charging effect is included. Although electrons and ions are continuously lost to the dust, it is possible to omit the loss terms by simply assuming that most of the electrons and ions recombine at the dust surface and the resulting atoms then re-enter the plasma and are re-ionized. One can either assume the existence of a source of ions and electrons to maintain the conservation of number densities or assume that

https://doi.org/10.1017/S002237780800706X Published online by Cambridge University Press

the production and loss cancel, which is a good approximation in the timescale of the wave variations. This 'standard dusty plasma model' including dust charge variations (with the inherent above-mentioned assumptions) has been widely used. From another angle, it is worth noting that we considered adiabatic dust charge variations (under the assumption that the ratio of dust charging time to the dust hydrodynamical time is very small) preventing therefore the non-adiabaticity-generated anomalous dissipative effects, which cause generation of collisionless shock waves. Of course, one can include some relevant processes inherent to the dust charge variation that can act concurrently (such as collisions, sources, and sinks). How can that affect our final results? The small-amplitude localized solitary structure becomes weakly dissipative in nature as was recently reported by Popel et al. [47], El-Labany et al. [64], and more recently by Ghosh [65]. Considering the wide relevance of nonlinear oscillations in laboratory and space dusty plasmas, our investigation may be taken as a prerequisite for the understanding of the different nonlinear features of localized electrostatic disturbances that may occur in a number of astrophysical dusty plasma systems, such as planetary ring systems, cometary environments, etc., where charge fluctuating dust grains and Boltzmann-distributed electrons and ions are the major plasma species. It may be stressed here that the time evolution and stability analysis of these solitary dust waves are problems of great importance but beyond the scope of the present work.

Acknowledgement

This work was supported in part by the Ministère de l'Enseignement Supérieur et de la Recherche Scientifique contract No. D00220060041.

References

[1] Goertz, C. K. 1989 *Rev. Geophys.* **27**, 271.
[2] Mendis, D. A. and Rosenberg, M. 1994 *Annu. Rev. Astron. Astrophys.* **32**, 419.
[3] Horanyi, M. 1996 *Annu. Rev. Astron. Astrophys.* **34**, 383.
[4] Verheest, F. 2000 *Waves in Dusty Space Plasmas*. Dordrecht: Kluwer.
[5] Shukla, P. K. and Mamun, A. A. 2002 *Introduction to Dusty Plasma Physics*. Bristol: IOP (and references therein).
[6] Selwyn, G. S. 1993 *Japan J. Appl. Phys.* **32**, 3068.
[7] Bliokh, P. V. and Yarashenko, V. V. 1985 *Sov. Astron.* **29**, 330.
[8] Shukla, P. K. 2001 *Phys. Plasmas* **8**, 1791.
[9] Merlino, R. L., Barkan, A., Thomson, C. and D'Angelo, N. 1998 *Phys. Plasmas* **5**, 1607.
[10] Rao, N. N., Shukla, P. K. and Yu, M. Y. 1990 *Planet. Space Sci.* **38**, 543.
[11] Shukla, P. K. and Silin, V. P. 1992 *Phys. Scr.* **45**, 508.
[12] Tribeche, M. and Zerguini, T. H. 2001 *Phys. Plasmas* **8**, 394.
[13] Mamun, A. A. and Gebreel, A. A. 2000 *Eur. Phys. J.* D **10**, 301.
[14] Tribeche, M., Houili, H. and Zerguini, T. H. 2002 *Phys. Plasmas* **9**, 419.
[15] Houili, H, Tribeche, M. and Zerguini, T. H. 2002 *J. Plasma Phys.* **67**, 115.
[16] Tribeche, M. 2005 *Phys. Plasmas* **12**, 072304.
[17] Tribeche, M., Ait Gougam, L., Aoutou, K. and Zerguini, T. H. 2005 *Phys. Plasmas* **12**, 092309.
[18] Tribeche, M., Ait Gougam, L. and Zerguini, T. H. 2007 *Phys. Scr.* **75**, 354.
[19] Shukla, P. K. and Stenflo, L. 2000 *Phys. Plasmas* **7**, 2738.

https://doi.org/10.1017/S002237780800706X Published online by Cambridge University Press

[20] Shukla, P. K., Stenflo, L. and Morfill, G. M. 2001 *IEEE Trans. Plasma Sci.* **29**, 198.
[21] Shukla, P. K., Stenflo, L., Mamun, A. A., Resendes, D. P. and Sorasio, G. 2002 *J. Geophys. Res.* **107**, 1293.
[22] Shukla, P. K. and Mamun, A. A. 2003 *Phys. Lett.* A **313**, 424.
[23] Shukla, P. K. and Eliasson, B. 2004 *Phys. Plasmas* **11**, 584.
[24] Shukla, P. K. and Mamun, A. A. 2004 *Phys. Plasmas* **11**, 1233.
[25] Mamun, A. A., Cairns, R. A. and Shukla, P. K. 1996 *Phys. Plasmas* **3**, 702.
[26] Mamun, A. A., Cairns, R. A. and Shukla, P. K. 1996 *Phys. Plasmas* **3**, 2610.
[27] Shchekinov, Y. A. 1997 *Phys. Lett.* A **225**, 117.
[28] Ma, J. X. and Liu, Jinyuan 1997 *Phys. Plasmas* **4**, 253.
[29] Tagare, S. G. 1997 *Phys. Plasmas* **4**, 3167.
[30] Mamun, A. A. 1998 *J. Plasma Phys.* **59**, 575.
[31] Mamun, A. A., Alam, M. N. and Azad, A. K. 1998 *Phys. Plasmas* **5**, 1212.
[32] Kakati, M. and Goswami, K. S. 1998 *Phys. Plasmas* **5**, 4508.
[33] Mamun, A. A. 1999 *Astrophys. Space Sci.* **268**, 443.
[34] Mamun, A. A. 1999 *Astrophys. Space Sci.* **260**, 507.
[35] Mamun, A. A., Russell, S. M., Mendoza-Briceño, C. A., Alam, M. N., Datta, T. K. and Das, A. K. 2000 *Planet. Space Sci.* **48**, 163.
[36] Mendoza-Briceño, C. A., Russell, S. M. and Mamun, A. A. 2000 *Planet. Space Sci.* **48**, 599.
[37] Das, G. C., Sarma, J. and Roychoudhury, R. 2001 *Phys. Plasmas* **8**, 74.
[38] Shukla, P. K. and Mamun, A. A. 2001 *IEEE Trans. Plasma Sci.* **29**, 221.
[39] Farid, T, Mamun, A. A., Shukla, P. K. and Mirza, A. M. 2001 *Phys. Plasmas* **8**, 1529.
[40] Ghosh, S., Sarkar, S., Khan, M. and Gupta, M. R. 2001 *IEEE Trans. Plasma Sci.* **29**, 409.
[41] Mamun, A. A. and Shukla, P. K. 2001 *Phys. Lett.* A **290**, 173.
[42] Mamun, A. A. and Shukla, P. K. 2002 *Phys. Scr.* **98**, 107.
[43] Mamun, A. A. and Shukla, P. K. 2002 *Geophys. Res. Lett.* **29**, 1870.
[44] Mamun, A. A. and Shukla, P. K. 2002 *Phys. Plasmas* **9**, 1468.
[45] Ghosh, S., Sarkar, S., Khan, M. and Gupta, M. R. 2002 *Phys. Plasmas* **9**, 1150.
[46] Mamun, A. A. and Shukla, P. K. 2002 *IEEE Trans. Plasma Sci.* **30**, 720.
[47] Popel, S. I., Golub, A. P., Losseva, T. V., Ivlev, A. V., Khrapak, S. A. and Morfill, G. 2003 *Phys. Rev.* E **67**, 056402.
[48] El-Labany, S. K., El-Taibany, W. F., Mamun, A. A. and Moslem, W. M. 2004 *Phys. Plasmas* **11**, 926.
[49] Li, Yang-fang, Ma, J. X. and Li, Jing-ju 2004 *Phys. Plasmas* **11**, 1366.
[50] Cairns, R. A., Mamun, A. A., Bingham, R., Boström, R., Dendy, R. O., Nairn, C. M. C. and Shukla, P. K. 1995 *Geophys. Res. Lett.* **22**, 2709.
[51] Mamun, A. A., Cairns, R. A. and Shukla, P. K. 1996 *Phys. Plasmas* **3**, 2610.
[52] Mamun, A. A. 1997 *Phys. Rev.* E **55**, 1852.
[53] Mamun, A. A. 2000 *Eur. Phys. J.* D **11**, 143.
[54] Mamun, A. A., Russel, S. M., Mendoza-Briceño, César A., Alam, M. N., Datta, T. K. and Das, A. K. 2000 *Planet. Space Sci.* **48**, 163.
[55] Mendoza-Briceño, César A., Russel, S. M. and Mamun, A. A. 2000 *Planet. Space Sci.* **48**, 599.
[56] Bandyopadhyay, A. and Das, K. P. 2000 *Phys. Plasmas* **7**, 3227.
[57] Chen, F. F. 1965 *Plasma Diagnostic Techniques* (ed. R. H. Huddlestone and S. L. Leonard). New York: Academic, ch. 4.
[58] Barnes, M. S., Keller, J. H., Forster, J. C., O'Neill, J. A. and Coultas, D. K. 1992 *Phys. Rev. Lett.* **68**, 313.

https://doi.org/10.1017/S002237780800706X Published online by Cambridge University Press

[59] Ma, J. X. and Yu, M. Y. 1995 *Phys. Plasmas* **2**, 1343.
[60] Whipple, E. C. 1981 *Rep. Prog. Phys.* **44**, 1198.
[61] Ma, J. X., Liu, Jin-yuan and Yu, M. Y. 1997 *Phys. Rev.* E **55**, 4627.
[62] Liu, Jin-yuan and Ma, J. X. 1997 *Phys. Plasmas* **4**, 2798.
[63] Rao, N. N. 1999 *Phys. Plasmas* **12**, 4414.
[64] El-Labany, S. K., Moslem, W. M. and Moslem, A. E. 2003 *Phys. Plasmas* **11**, 4217.
[65] Ghosh, S. 2005 *J. Plasma Phys.* **71**, 519.

https://doi.org/10.1017/S002237780800706X Published online by Cambridge University Press